EUROfusion

EUROFUSION WPDIV–PR(15)04

J–H. You et al.

A Brief Review on Two Previous Divertor Target Concepts for DEMO: Mutual Impact between Structural Design Requirements and Materials Performance

Preprint of Paper to be submitted for publication in
Nuclear Fusion

This work has been carried out within the framework of the EUROfusion Consortium and has received funding from the Euratom research and training programme 2014-2018 under grant agreement No 633053. The views and opinions expressed herein do not necessarily reflect those of the European Commission.

A brief review on two previous divertor target concepts for DEMO: Mutual impact between structural design requirements and materials performance

Jeong-Ha You

Max Planck Institute for Plasma Physics, Boltzmann Str. 2, 85748 Garching, Germany

*Contact
e-mail: you@ipp.mpg.de
Phone: ++49 (0)89 3299 1373
Fax: ++49 (0)89 3299 1212

Abstract

Development of a diverter target with a sufficient capability of power exhaust is a crucial prerequisite for the realization of a fusion power plant. While the design and technology for divertor target has been successfully developed for ITER, the applicability of this concept is not necessarily assured yet for DEMO mainly because the neutron irradiation dose expected for DEMO divertor will be by an order of magnitude higher than that of the ITER divertor. The possible embrittlement of structural heat sink materials due to irradiation may restrict the performance and the operational flexibility of a target component to a considerable extent. In this article, the mutual impact between the design requirements and the operational limitation of structural materials. Water-cooled and helium-cooled concepts are discussed considering two representative heat sink materials, CuCrZr alloy and oxide-doped tungsten, respectively. In the case of water-cooled target the maximum allowable coolant temperature defined by the thermo-hydraulic requirement was applied as fundamental design constraint. On the contrary, the safe operational temperature window of structural heat sink was considered as paramount design constraint. Conclusions are derived from the critical features of heat sink performance in terms of structural reliability, design/material interface and further R&D needs.

Keywords: DEMO, divertor, high-heat-flux loads, water-cooled target, helium-cooled target, structural design

1. Introduction

Since a decade, conceptual design activities for a demonstration fusion reactor (DEMO) have been worldwide initiated and carried out posing new challenges for fusion power. Recently, a conceptual design program for the European DEMO was launched in the framework of the EUROfusion Consortium, a European joint undertaking for integrated fusion R&D programs based on the roadmap of Horizon 2020 [1]. In this program, the capability of reliable power handling was declared as one of the crucial prerequisites for the realization of a commercially viable fusion power plant. In this context, the development of the plasma-facing component (PFC) of diverter is a serious engineering challenge, since the harsh loading environment in a DEMO reactor is expected to produce extreme thermal, mechanical and physical impacts on the divertor PFC leading to damage and degradation of materials [2]. The PFC of a divertor cassette consists of three parts, namely, vertical target, dome and baffle. The typical structure of a divertor cassette is illustrated in Fig. 1 showing the early version of the CAD model of a DEMO divertor cassette [3].

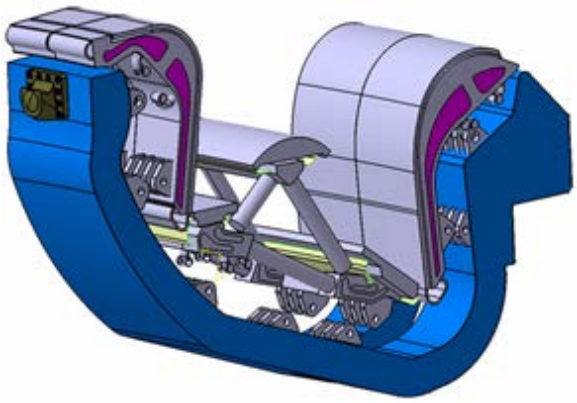

Fig. 1. Early version of the CAD model of the DEMO divertor cassette [3].

The PFC of the divertor is a high-heat-flux (HHF) component which is to be subjected to variable heat flux loads. The profile of the heat flux load on the divertor target plate sharply peaks at the narrow band of strike line. This peak heat flux is one of the fundamental design parameters of a tokamak as it is directly related to the power exhaust balance. It is restricted by the heat removal capability of the divertor PFC among others. The technology of divertor PFC has been successfully developed and qualified for ITER. It was already demonstrated that a prototype PFC fabricated with a state-of-the-art technology could survive at least 5,000 load cycles at 10 MW/m² and 300 cycles at 20 MW/m² thus fulfilling the design life of ITER [4, 5]. The relatively large heat removal capability of the ITER divertor target is owing to the water-cooling concept.

In the conceptual design of European DEMO, the water-cooled ITER-like divertor target design was adopted as baseline design concept assuming that the HHF loads expected for the DEMO divertor would be comparable to that of the ITER divertor [6]. On the other hand, helium-cooled design concept has been also developed as alternative design option in parallel to the water-cooled one [7]. Provisionally, it is assumed in this paper that the peak heat flux load on the DEMO divertor target ranges between 10 and 15 MW/m² during the steady state normal operation and can reach up to 20 MW/m² under slow transients. The question as to whether the design and technology of the ITER-like divertor target can be extrapolated to the DEMO divertor operation condition is currently still open. The reason of this uncertainty is mainly related to the fact that the neutron irradiation dose expected for the DEMO divertor PFC could be by an order of magnitude higher than that of the ITER and thus causing more severe embrittlement of the structural material. Such embrittlement restricts the operational performance of the PFC to a considerable extent [2].

The type of coolant and the thermohydraulic cooling condition are the fundamental design factors of the divertor PFC. They are derived from the envisaged maximum power exhaust goal. The resulting operation temperature range of the divertor target has a direct impact on the materials selection, in particular for the heat sink, which has to fulfill the structural design criteria. For structural design, it should be noted that the degree of irradiation effects (e.g. embrittlement) normally depends on temperature and may even vanish, when the temperature is sufficiently high owing to thermal recovery. Therefore, a careful definition of operation temperature is desired to enable loading of structural material in a ductile state.

A similar consideration is needed for design, when tungsten is used as structural material of a divertor target. Like some other body-centered cubic crystals, tungsten exhibits a ductile-to-brittle transition (DBT) behavior as well. It is advised to operate a tungsten heat sink above the DBT temperature (DBTT) in order to avoid brittle failure. Obviously, this rule can only be met by high-temperature gas cooling. It is noted that DBTT generally tends to be elevated by irradiation.

The circumstance discussed above clearly indicates that there are mutual influences between thermal/mechanical performance of heat sink materials, irradiation effects, cooling condition and structural design requirements.

The aim of this article is to review two representative divertor target concepts, namely, the water-cooled ITER-like target and the helium-cooled multi-jet impingement modular finger target and to elucidate the multisided relationship between design and material issues.

2. Loads imposed upon the divertor target

The essential function of the divertor is to remove the boundary plasma in the scrape-off layer by magnetic detraction and thus to control the concentration of the helium ash and the impurities sputtered from the wall. The incident plasma particle flux on the target surface is predicted to be in the order of $10^{24}/(m^2\ s)$ at heat flux of 10 MW/m² and radiative dissipation of 25% [7]. Such intensive bombardment of energetic particles can cause severe erosion on the armor surface limiting the functional lifetime of the target [8, 9].

In addition, strong thermal power of a megawatt range is generated on the armor surface. The distribution of the heat flux on the target is highly inhomogeneous peaking at the narrow band of strike zone (width: several mm) [7, 10]. The peak heat flux load to be produced on the DEMO divertor target is currently not determined yet, since it depends on a number of undefined operational factors such as the radiation power from the core, local radiative cooling of divertor plasma and the stability of plasma detachment, etc. [7, 10]. In this paper, it is assumed as discussion basis that the maximum heat flux load on the DEMO divertor is 10 MW/m² in the steady state and 20 MW/m² during slow transient (plasma reattachment) phase, respectively.

The fraction of thermal power to be exhausted through the divertor amounts roughly to 18 % of the total fusion power. As the amount of fusion power scales with the radius of a tokamak to the third power, the demand of power exhaust through the divertor target increases rapidly with reactor size. For ignition, the major radius of DEMO will have to be at least as large as 7 m [11].

Additionally, short transient events caused by plasma instability will need to be considered for DEMO PFC as in ITER in case effective mitigation tools should not be available [12]. The most prominent instability modes are edge localized mode (ELM: ~1 MJ/m², <1 ms, ~1 Hz) and plasma disruption (~10 MJ/m², ~1 ms) [7, 10]. The repeated ELM loads can produce detrimental and irreversible damages on the armor surface (e.g. cracking, plastic damage, melting) depending on the armor temperature [13-15]. On the contrary, radiation and neutron volumetric heating would have only minor contribution to the total heat flux to be deposited on the target [7].

In DEMO, neutron irradiation would pose substantially more critical problems for materials compared to ITER [16]. Irradiation is known to produce lattice defects in materials leading to embrittlement and reduced thermal conductivity. Helium bubble production by transmutation is another negative consequence which would affect the strength and ductility of materials negatively [17]. The irradiation dose on the divertor PFC will be distributed non-uniformly.

The strike zone of target would be exposed to much less dose compared to the other parts of the divertor PFC such as the dome or baffle owing to partial shielding. According to a recent neutronic calculation, the dose rate on the divertor target is estimated to range between 2-6 dpa per fpy (full power year) in the tungsten armor and 3-10 dpa per fpy in the Cu alloy heat sink [17].

The irradiation-induced embrittlement poses a particularly critical problem with regard to the structural reliability of the PFC. In the structural design practice, the operation temperature range for the heat sink should be chosen on the basis of optimal compromise between the degree of thermal recovery of damage and the capability of heat removal.

3. Material requirements for the heat sink

To develop an appropriate structural material for the divertor heat sink is one of the major engineering challenges. Following properties should be fulfilled as much as possible:

- high thermal conductivity
- high strength and toughness at elevated temperatures
- ductility and machinability
- sufficient fatigue life
- watertightness (in case of water-cooling)
- corrosion resistance
- moderate activation level acceptable for recycling
- moderate swelling
- low helium transmutation rate
- moderate irradiation effect and ability of damage recovery
- low tritium solubility
- good wettability to armor material (e.g. tungsten)
- sufficiently high melting point
- Availability and reasonable cost

Surely, such a long list of diverse requirements can be hardly satisfied by a single material. The paramount priority needed for the heat sink is high thermal conductivity among others.

Fig. 2 shows a schematic illustrating the screening procedure for heat sink materials for the given selection criteria (vide supra). Only the most important criteria are considered (see the legend). In this schematic a set of pure solid elements with thermal conductivity higher than 50 MW/mK are arrayed. In the box of each element the corresponding thermal conductivity value is given together with the element symbol, respectively [18]. The elements are arrayed in an

ascending order of thermal conductivity. The grey-shaded boxes indicate the elements that fail to meet at least one or two of the given criteria. The 'failed' item(s) of the criteria is (are) also indicated on the top of the individual boxes.

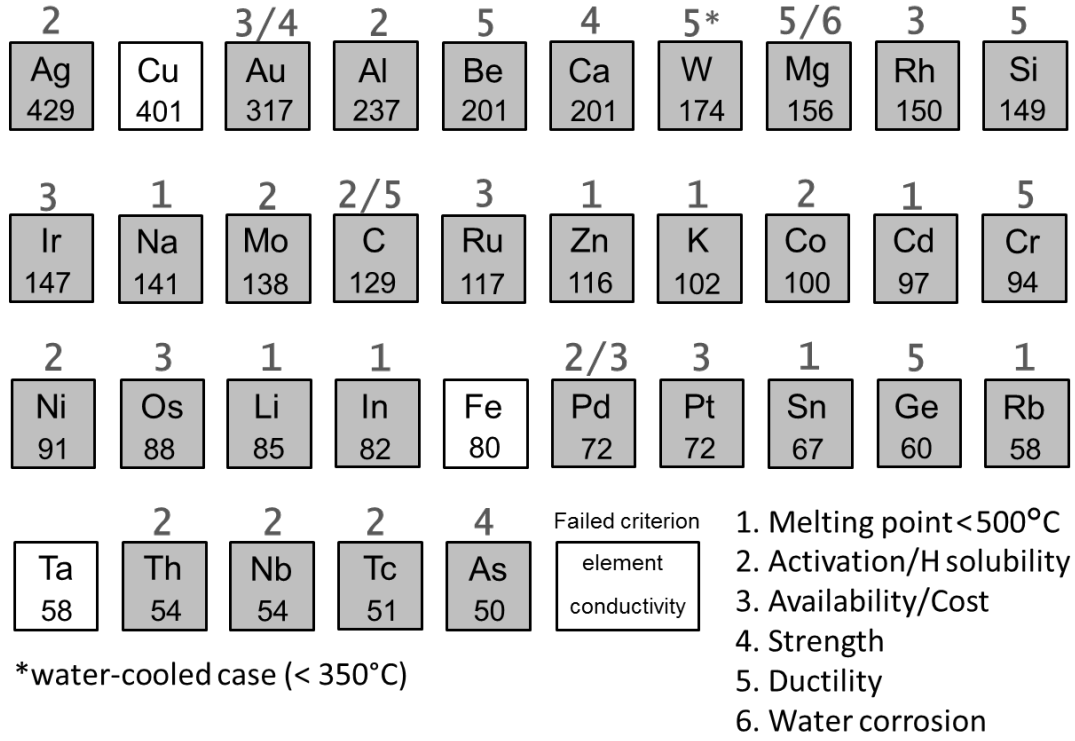

Fig. 2. Pure materials in solid state which possess thermal conductivity higher than 50 MW/mK. In each box the value of conductivity is given. The grey-shaded boxes indicate the materials that fail to meet at least one or two of the criteria. The 'failed' item of the criteria is indicated on the top of the individual boxes, respectively.

It is seen that for a low-temperature target concept based on water-cooling only three metals (copper, iron and tantalum) may come into question without essential deficiency. It is noted that iron is normally used as steel and steels have much lower conductivity than iron. (NB: the thermal conductivity of Eurofer is about 30 W/mK) [2]. Furthermore, both ferritic steels and tantalum exhibit a DBT behavior as BCC metals. In order to avoid brittle failure the operation temperature of the heat sink needs to be placed above the DBTT by increasing the coolant temperature accordingly. In case of water-cooling, the coolant temperature cannot be elevated to 250-300 °C due to the limitation of heat removal capability. In this circumstance tungsten does not come into question for the heat sink, because the temperature will surely be much lower than the DBTT. Therefore, copper alloys seem to be the best and probably the only candidate material group for the heat sink of a water-cooled target, at least from the thermal point of view.

The activation issue of copper is relatively moderate, although copper is often regarded as being medium-activating. Copper with a dose of up to 20 dpa reaches the class of low level waste after decay time of 100 years [16]. This decay rate seems to be compatible with one the requirements of DEMO, namely, recyclability. Pure copper shows rather strong swelling, but copper alloys (e.g. CuCrZr) tend to exhibit a much reduced swelling and He production. For instance, even at the high dose of 150 dpa, the maximum swelling of CuCrZr alloy at 410 °C was reported to be lower than 2 % [16].

In the case of high-temperature divertor target concepts based on helium-cooling, tungsten has been considered as the most promising heat sink material. But the structural applicability of tungsten depends on the successful metallurgical development aiming at a reduced DBTT and enhanced toughness even under irradiation. Sufficient amount of reliable irradiation test data will be the most urgent need for the structural design of a tungsten heat sink.

4. Irradiation effects on the mechanical performance.

Hardening, embrittlement and creep belong to the most pronounced mechanical effects of irradiation. These effects normally exhibit significant temperature-dependence and thus are likely to be affected by operation conditions. In the following, we discuss this issue for two baseline heat sink materials: CuCrZr alloy (water-cooled) and tungsten (helium-cooled).

4.1. CuCrZr alloy for water-cooled heat sink

The strength of CuCrZr alloy comes from the Orowan mechanism activated by dislocation interaction with finely distributed intermetallic precipitates and the small dislocation loops produced by neutron cascade [19]. The capability of global ductile elongation of irradiated CuCrZr alloy is substantially limited by the microscopically localized long-range mobility of dislocations through narrow defect-free channels (so-called cleared channeling) which leads to a concentrated plastic flow on a microscopic scale while the apparent ductility is reduced on a macroscopic scale [19, 20].

Fig. 3 shows the uniform elongation data of CuCrZr alloy measured at a temperature range between 100 and 350 °C after neutron irradiation to 1-10 dpa. The data were collated from several irradiation test reports found in literature [21-24]. Here, the test temperature was set equal to the irradiation temperature. The data plot reveals that the CuCrZr alloy irradiated and tested at or above 250 °C exhibits a clear thermal recovery effect. On the contrary, the uniform elongation is marginal (< 2%) when irradiated below 250 °C. Should the uniform elongation limit be considered as structural criterion, then the cooling tube made of CuCrZr alloy might be

subject to a strict operational restriction with regard to temperature in order to avoid embrittlement. It is widely accepted as a prudent engineering practice to base the structural design of a nuclear component upon ductile operation regime. From this point of view, the transition temperature of 250 °C may be regarded as the lower limit of operation temperature for the CuCrZr alloy cooling tube.

On the other hand, setting coolant temperature to 250 °C will unduly restrict the heat removal capability of a target under slow transient events. A sufficient margin to the critical wall heat flux can only be assured by keeping the coolant temperature sufficiently low (below 150 °C). The question of how to determine the lower bound operation temperature for the heat sink is directly related to the trade-off problem between heat removal capability and embrittlement of the heat sink material.

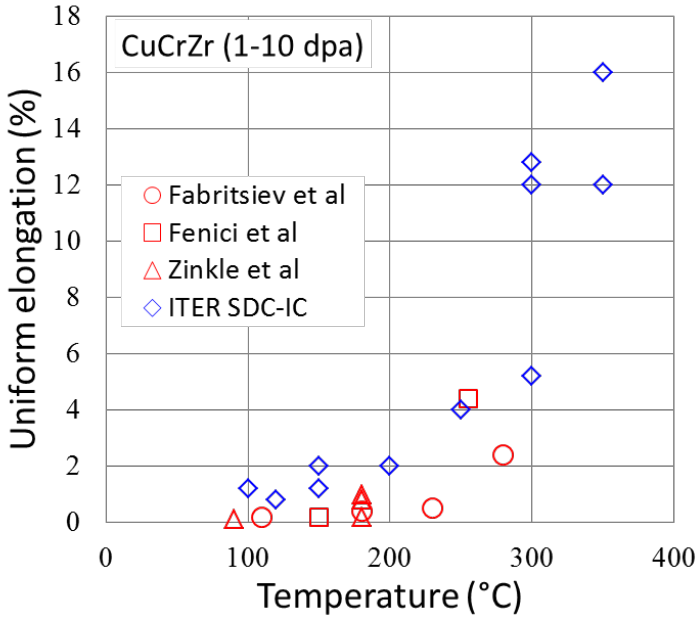

Fig. 3 Uniform elongation data of CuCrZr alloy irradiated to 1-10 dpa plotted as a function temperature. The data were collated from several different test reports published in literature [21-24].

Uniform elongation regime is terminated by plastic necking. In the structural design criteria of the ITER in-vessel components (ITER SDC-IC), the design rule against the failure by necking is defined as a criterion for immediate plastic flow localization (during irradiation) [24]. This criterion is formulated in terms of either the stress limit S_e (elastic analysis) or the maximum uniform strain (plastic analysis). Unfortunately, such a mature design code is not available yet for the DEMO divertor. As CuCrZr alloy exhibits an early saturation behavior with regard to

irradiation effects [16], the stress limit data collated in the SDC-IC code can be used as a guideline for the DEMO divertor (water-cooled) as well.

In ITER SDC-IC code there is another failure criterion that can be affected by embrittlement as well, namely, immediate local fracture due to exhaustion of ductility. This type of failure is related to the stress limit S_d (elastic analysis) or the total ultimate tensile strain (plastic analysis). In contrast to the uniform elongation limit which almost vanishes under irradiation at low temperatures, CuCrZr alloy preserves still extensive total elongation even under cold irradiation as shown in Fig. 4.

Fig. 4 shows the tensile curves of precipitation-hardened CuCrZr alloy measured before and after irradiation up to 10 dpa at 150 °C and 250 °C, respectively, in fast neuron reactors. [22]. Here, the same temperature was set for testing and irradiation. A strong hardening effect is found together with conspicuous embrittlement after irradiation at 150 °C. Here, the uniform elongation is negligibly small while the total elongation is still quite considerable (roughly 8 %). On the contrary, the irradiation and test at 250 °C does not seem to affect the ductility of CuCrZr alloy, although slight hardening is discernable. These test data confirm again that irradiation at or above 250 °C will not pose any structural issue of embrittlement for the CuCrZr heat sink. Rather, the slight hardening by irradiation should have even a beneficial effect, as the design stress limit S_m is increased.

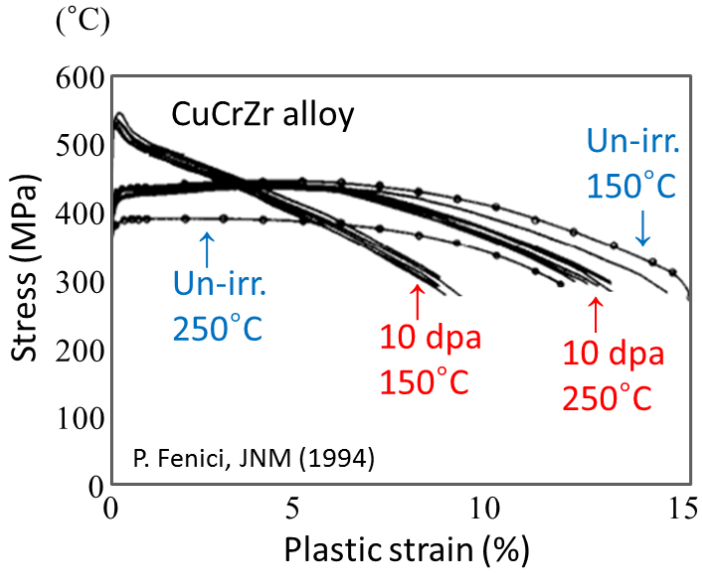

Fig. 4 shows the tensile curves of precipitation-hardened CuCrZr alloy measured before and after irradiation to 10 dpa at 150 °C and 250 °C, respectively (each test temperature is equal to the irradiation temperature) [22].

The irradiation data at 150 °C requires careful scrutiny. The Cu alloy irradiated at 150 °C can still undergo considerable plastic deformation (up to 8 %) before rupture, although the onset of necking occurs immediately after yield indicating negligible uniform plastic deformation. In the heat sink tube, stress is generated mostly by thermal strains due to the mismatch in differential thermal expansion. In such a strain-controlled loading condition, the heat sink will be loaded only up to a well-defined strain range and not necessarily to ultimate rupture even after local necking. In the case of the conventional ITER-like W monoblock design, the maximum total strain in the CuCrZr alloy tube is estimated to be about 1.2 % (see Fig. 12) which is much smaller than the ultimate tensile rupture strain (8 %). Thus, it is thought that the CuCrZr tube would be able to withstand stationary HHF loads even under cold irradiation at 150 °C.

The tensile curves of irradiated CuCrZr alloy at 150 °C exhibit a diminishing plastic strength (softening) after necking. But, this softening behavior would not be a major issue, when the maximum tensile plastic strain is limited to 1-2 % under strain-controlled loading.

The ITER SDC-IC code provides with the elaborated data of design stress limits of irradiated CuCrZr alloy. Selected design stress limits are plotted in Fig. 5 as a function of temperature. The subscript ‘irr’ and ‘unirr’ stands for the irradiated and pristine specimens, respectively.

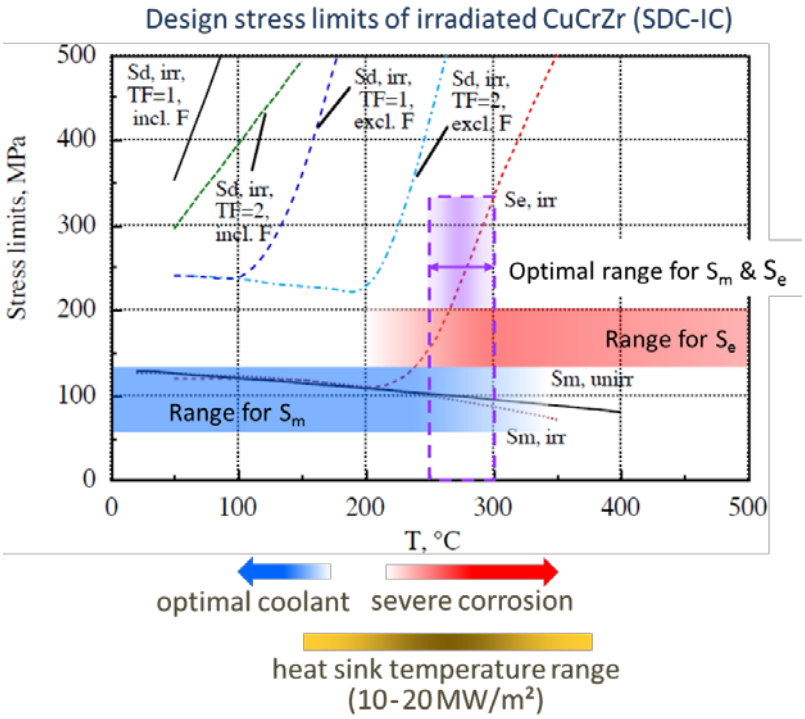

Fig. 5. Selected stress limits of CuCrZr alloy from the SDC-IC code plotted as a function of temperature. The subscript ‘irr’ and ‘unirr’ stands for the data of an irradiated and pristine specimen, respectively [24].

This diagram indicates that the elastic structural design rules would allow only a narrow window of operation temperature (250 - 300 °C) for the cooling tube, if CuCrZr alloy shall be used as heat sink material. On the other hand, the relatively high lower temperature limit required by ductile structural design (i.e. T ≥ 250 °C) may possibly cause a serious problem of corrosion-erosion depending on the water chemistry, wall temperature and coolant speed [25-27]. The most critical consequence of such a rather high coolant temperature is, however, the fact that the thermal redundancy to the critical heat flux under off-normal loads becomes too tight. This conflicting circumstance manifests the trade-off between the structural design requirements on one hand (ductile design) and the functional performance of the structural material on the other (reduced corrosion, heat removal capability).

This dilemma could be resolved, if the elastic design criterion based on S_e limit is abandoned and the plastic total elongation criterion is employed instead, while accepting a small amount of necking to be caused by irradiation embrittlement. In this case low-temperature operation of water coolant (say, T ≤ 150 °C) can be allowed. This design approach could be justified by the experimental observation that the fracture toughness of cold-irradiated CuCrZr alloy (80 °C, 1 dpa) exhibits only little decrease compared to un-irradiated one as shown in Fig. 6 [22]. The irradiation damage of the CuCrZr heat sink could be partially recovered by means of in-situ heat treatment during maintenance phase using warm helium gas [28].

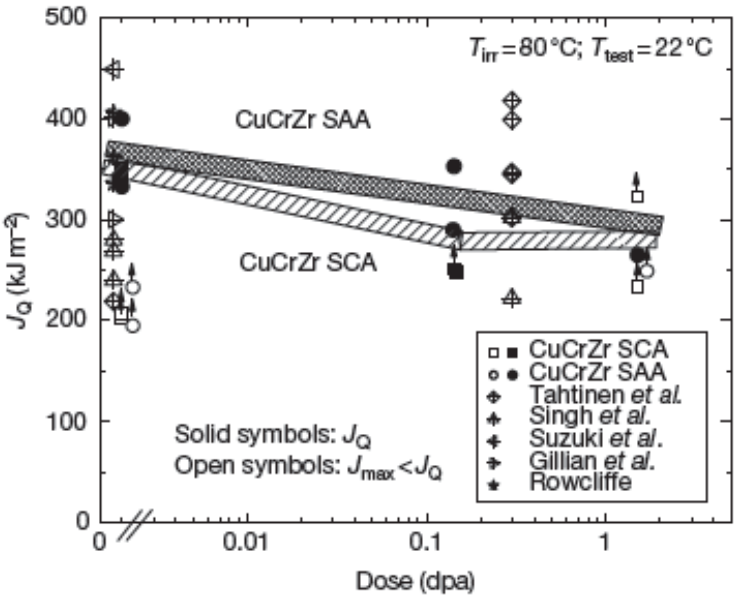

Fig. 6. Fracture energy of cold-irradiated (80 °C) CuCrZr alloy with two different kinds of heat treatment as a function of irradiation dose (SAA: solution-annealed & prime aged, SCA: slow-cooled & aged) [22].

4.2. Tungsten for helium-cooled heat sink

For helium-cooled divertor target, tungsten (or W alloys) has been the exclusively preferred structural material for the heat sink. However, there is a fundamental concern for tungsten as structural material that commercial grade tungsten materials are generally afflicted with the critical issues of inherent brittleness below DBTT and nuclear embrittlement (dpa damage and transmutation leading to formation of brittle phases). A recent irradiation campaign for tungsten conducted in a thermal neutron source showed that severe embrittlement took place even in the early stage of dpa damage [29]. The situation will be aggravated in the actual fusion operation by the much higher kinetic energy of impinging neutrons.

The fracture energy measured in a Charpy impact test is often used as a measure of ductility. Fig. 7 shows the data of Charpy impact tests obtained for tungsten (W), lanthanum oxide-doped tungsten (WL10), Eurofer steel (9Cr-1WVTa) and a molybdenum alloy (TZM) [30]. Here, the energy consumed for breaking a specimen by an impact load is plotted over the test temperatures. The temperature band indicating the increase of energy of individual materials defines the DBTT, respectively. It is seen that the DBTT for W and WL10 ranges from 800 to 950 °C. The DBTT values will be shifted to higher temperatures, when irradiated.

As tungsten has a negligible ultimate tensile elongation below DBTT (<1-2 %) with no post-necking deformation [31], there will be no plastic resilience, when the operation temperature is lower than the DBTT. This is in contrast to the case of CuCrZr alloy.

The fairly high DBTT of tungsten imposes challenging restrictions on the structural design of a helium-cooled target. In order to avoid a catastrophic brittle failure, a sufficient temperature margin to DBTT is desired.

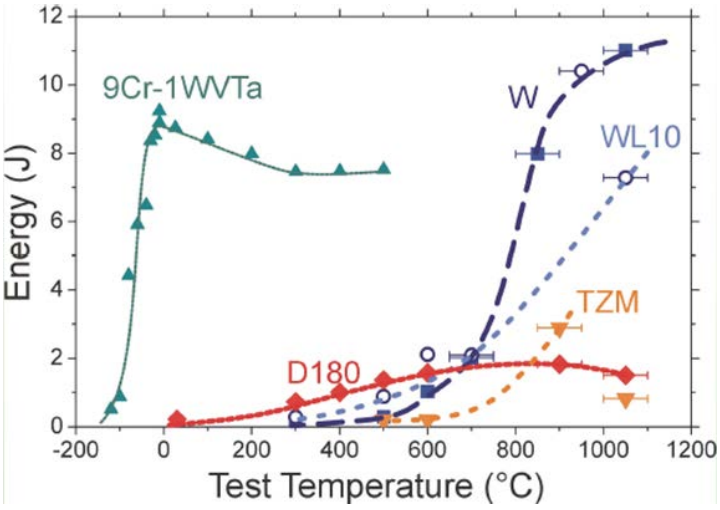

Fig. 7. Data of Charpy impact tests conducted for pure W, La oxide-doped tungsten (WL10), a reduced-activation steel (9Cr-1WVTa) and a Mo alloy (TZM) [30].

4. Water-cooled target

One of the candidate design concepts currently considered for the water-cooled divertor target of DEMO is the ITER-like target model consisting of tungsten monoblocks joined to a CuCrZr cooling tube with a Cu interlayer. A test mock-up of a typical ITER target element is shown in Fig. 8 as an example [13]. In order to make a prediction as to whether the heat sink tube will be operated in ductile regime, one needs to estimate the temperature response of the tube for the relevant combinations of HHF load and cooling condition. In the following the results of a parametric finite element analysis (FEA) are discussed.

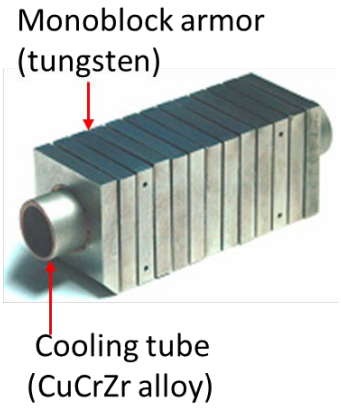

Fig. 8. Mock-up of an ITER divertor target element consisting of tungsten monoblocks joined with a CuCrZr cooling tube via a Cu interlayer [13].

The geometry (symmetric half) of an ITER-like target considered for FEA is illustrated in Fig. 9. The W armor block has a dimension of 23×22×4 mm^3. The CuCrZr tube has a thickness of 1 mm with an inner diameter of 12 mm. The thickness of the Cu interlayer is 0.5 mm.

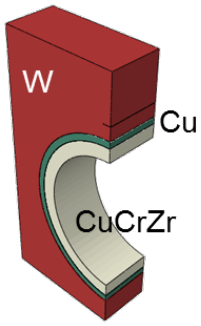

Fig. 9. Schematic of the FEA model (symmetric half) considered for FEA. W armor block: 23 mm×22 mm×4 mm, cooling tube thickness: 1 mm, inner diameter: 12 mm, Cu interlayer thickness: 0.5 mm.

Fig. 10 shows an example of temperature field produced in the cooling tube (only the left half is shown) calculated for the heat flux load of 15 MW/m² and coolant temperature of 200 °C. The arrows indicate the two locations at which temperature is examined. These two sites correspond to the upper and lower boundary of the most stressed region of the tube as illustrated in the thermal stress field in Fig. 11 which shows the circumferential component in a cylindrical coordinate system.

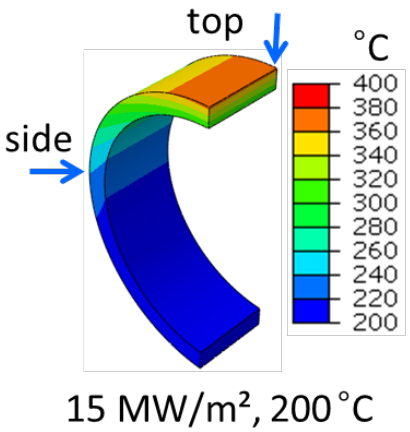

Fig. 10. Temperature field in the cooling tube (left half part) predicted for the heat flux load of 15 MW/m² and coolant temperature of 200 °C. The two locations are indicated for which the temperature values are presented [32].

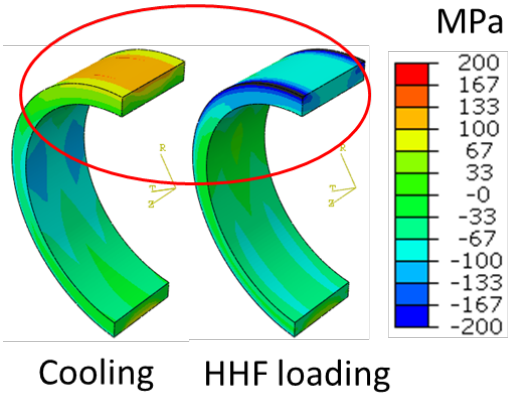

Fig. 11. Circumferential component of the thermal stress field produced in the cooling tube after 10 load cycles (heat flux load: 15 MW/m², coolant temperature of 200 °C).

The temperature values at the two selected locations are listed in Table 1 [32]. Six different load cases were simulated considering the combinations of three heat flux loads (10, 15 and 18 MW/m²) and two coolant temperatures (150 and 200 °C). In Table 1, the temperature data of

the cooling tube are grouped in two categories, namely, possibly permissible (grey) and not permissible (white) for stationary operation. Here, following criteria were considered:

1) upper temperature limit at the top: 320 °C (irradiation creep for highly stressed region)
2) lower temperature limit at the top: 230 °C (brittleness for highly stressed region)
3) upper temperature limit at the inner wall: 200 °C (corrosion with protection coating)
4) lower temperature limit at the side: 150 °C (brittleness for moderately stressed region)

It is noted that these criteria were derived by the subjective judgment of the present author on an interim basis assuming rather relaxed material requirements.

Table 1. Temperatures (°C) at two selected locations of the cooling tube computed by FEA.

Heat flux load	10 MW/m²		15 MW/m²		18 MW/m²	
Coolant water	150	200	150	200	150	200
Tube top bond interface	263	308	316	351	348	378
Tube top inner wall	229	274	266	300	288	317
Tube side bond interface	172	220	181	228	187	233
Tube side inner wall	169	217	177	225	182	229

This screening study reveals that none of the considered load cases can fully meet the four criteria stated above. In all load cases, the maximum temperature of the tube wall violates the allowable limit required for avoiding severe corrosion. Provided that a successful corrosion protection technology can be developed, then one might achieve a stationary heat flux load of 10 MW/m² or higher with a cold coolant temperature at or below 150 °C. The final judgment as to whether or not the predicted temperatures are permissible for structural application can be delivered by checking the relevant structural design criteria for the respective load cases. The constraint on coolant temperature imposed by corrosion issue ($T \leq 150$ °C) also matches the fundamental thermo-hydraulic requirement derived from the demand on power exhaust capability.

The maximum allowable temperature and thus the HHF performance are limited by thermal softening and irradiation creep. In this context, the interplay between the plastic strength of the tube at upper operation temperatures and the stress state (in particular the residual stress) plays an important role in plastic failure behavior such as low cycle fatigue or ratchetting.

Fig. 12 shows the plastic strain fields in the CuCrZr tube after 10 HHF load cycles under 15 MW/m² (coolant temperature: 200 °C). Plotted are the circumferential (left) and axial (right) strain component. It is seen that the plastic strain is concentrated at the free surface edge of the bond interface up to 1.2 % while the bulk volume of the tube experiences rather moderate uniform plastic deformation up to 0.6 %. It should be noted that the plastic deformation is produced entirely during the fabrication process (i.e. during cooling after joining) and no more during the subsequent HHF loading.

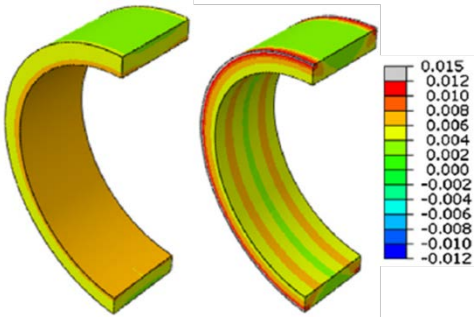

Fig. 12. Circumferential (left) and axial (right) component of the plastic strain in the cooling tube after 10 load cycles (heat flux load: 15 MW/m², coolant temperature of 200 °C) [32].

This rather surprising feature is demonstrated in Fig. 13 where the history of three principal plastic strain components in the cooling tube bulk is plotted during the HHF load cycles. The strain components are given for a cylindrical coordinate system. In this FEA simulation, the fabrication process and pre-heating to standby state are also considered [32]. The plot shows clearly that plastic deformation ceases once the pre-heating is completed and that no further plastic straining occurs in the following HHF load cycles. The stress states in the CuCrZr tube enters into the state of elastic shakedown which means a safe operation regime from the structural point of view. It is recalled that the embrittlement issue of the CuCrZr tube is only related to the HHF loading stage, but not to the fabrication process or preheating. Therefore, the plastic failure criteria based on uniform as well as total elongation limit of cold-irradiated CuCrZr alloy would never be violated. This feature is also valid for lower HHF loads and lower coolant temperatures as well, since the residual stress produced by the same fabrication process overwhelms the secondary stresses in each HHF load case.

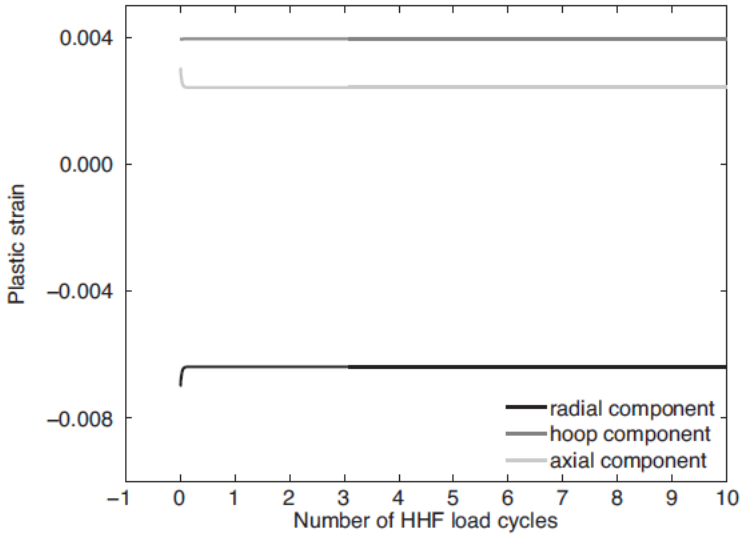

Fig. 13. History of the principal plastic strain components in the cooling tube bulk during the HHF load cycles (cylindrical coordinate system). The fabrication process and pre-heating to standby state are also considered [32].

It should be noted that the final plastic strength of CuCrZr alloy can vary quite sensitively depending on the previous temperature history or thermo-mechanical treatment [33]. Thus, the strength of a CuCrZr tube embedded in a full-size prototypical target may possibly have a considerably reduced strength (say, 60 %) due to limited or omitted prime-ageing treatment. This effect could cause cyclic plastic deformation during HHF loading leading to low cycle fatigue. Hence, it is urgently desired to develop novel heat sink materials which possess both enhanced high-temperature strength and excellent heat conductivity [34, 35].

The message delivered by the result given in Fig. 13 seems obviously optimistic, when only the heat sink tube is considered for structural design. Note that tungsten armor does not need to fulfill the structural design rules in the sense of SDC-IC as functional member, although cracking and fracture of tungsten armor turned out to be highly probable under slow transient loads and can be problematical from the structural integrity point of view [36, 37].

In a similar way to the tungsten armor, the soft copper interlayer can be a potentially critical weak site. Fig. 14 shows the history of the principal plastic strain components in the copper interlayer during the HHF load cycles after fabrication and pre-heating [32]. One finds that periodic fluctuation of plastic strain takes place with significant strain amplitudes during the HHF cycles. This response causes cyclic plastic dissipation and incremental accumulation of strain damage leading to a low cycle fatigue of the interlayer. The overall fatigue failure of the

copper interlayer could fatally affect the global integrity of the whole target system. The estimated fatigue life of the copper interlayer is approximately 26,500 load cycles in the bulk and 3,500 cycles at the edge under HHF load of 10 MW/m² and with coolant of 150 °C [32]. When the heat flux is increased to 15 MW/m², then the fatigue life is reduced to 10,500 and 1,200 cycles, respectively. The fatigue life could be further reduced by embrittlement due to helium production from transmutation. Unfortunately, the upper temperature range (350-400 °C) of the copper interlayer overlaps with that of maximum helium segregation [38].

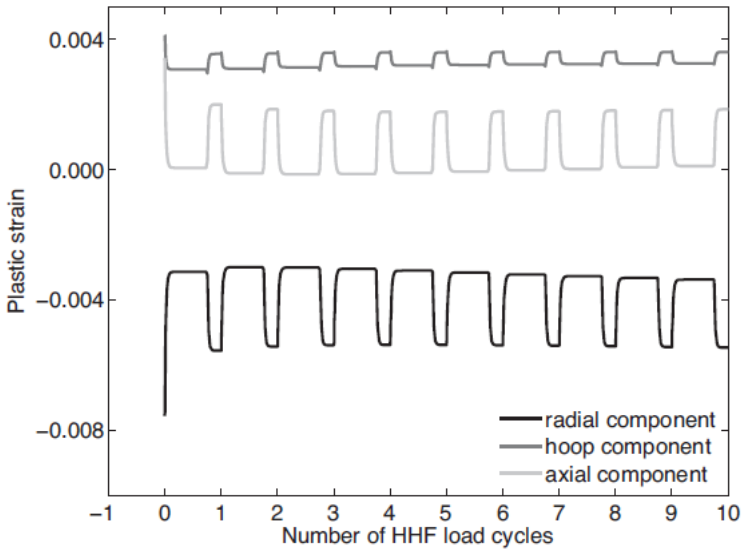

Fig. 14. History of the principal plastic strain components in the copper interlayer during the HHF load cycles. The fabrication process and pre-heating to standby state are also considered [32].

5. Helium-cooled target

Helium-cooled divertor target concepts have been developed in EU and US [7, 39]. Among others, the multi-jet impingement modular finger concept developed at the KIT in the last two decades is the most developed one. Hence, we'll discuss the design issues of this concept as an example in this chapter.

Fig. 15 shows the longitudinal cut section of a single finger module (right) together with a schematic illustration (left) [39]. Fig. 16 shows the heat sink (thimble) made of tungsten alloy (WL10). The thimble is a structural part to be subjected to pressurized jet of hot helium gas (600 - 700 °C, 100 bar). Therefore, the tungsten thimble has to fulfill relevant structural design criteria for the envisaged operation temperature window.

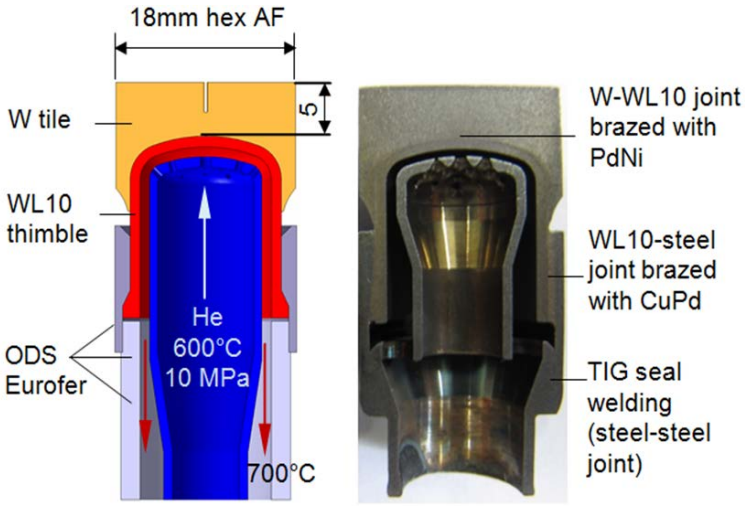

Fig. 15. Longitudinal section view of a multi-jet modular finger target unit with a schematic illustration (left) and photograph (right) [39].

Fig. 16. Heat sink (thimble) of the modular finger target made of tungsten alloy (WL10) which is subjected to pressurized hot helium gas (600 - 700 °C, 100 bar) [39].

The inlet temperature of the gas coolant was determined in such a way that the temperature of the highly stressed part of the thimble remains higher than the DBTT of the tungsten alloy so that the ductility of the pressurized thimble is preserved during HHF loading. One of the most critical concerns related to this target concept is the critical impact of neutron irradiation on the toughness of tungsten. Irradiated tungsten is known to exhibit increased DBTT. Should the DBTT of the structural tungsten material exceed the operation temperature range of the thimble due to irradiation, the pressurized heat sink would get into an unallowably brittle state. Hence, the temperature of the structural parts is an important design parameter.

Fig. 17 shows the temperature field in the finger module computed for a typical HHF load [39]. Only a rotational symmetric part is plotted (1/6 sector). The assumed heat flux was 10 MW/m² and the inlet coolant temperature was 600 °C (pressure: 100 bar). The resulting outlet helium temperature amounts to 700 °C. Consequently, the coldest part of the heat sink thimble located in the gas outlet region is heated up to 700 °C. As the steel casing is joined to the coldest part

of the thimble, the steel casing also has to withstand the outlet temperature of 700 °C. On the other hand, the hot spot of the thimble is heated up to 1175 °C whereas the most stressed part of the thimble only to 880 - 970 °C being just in the range of DBTT.

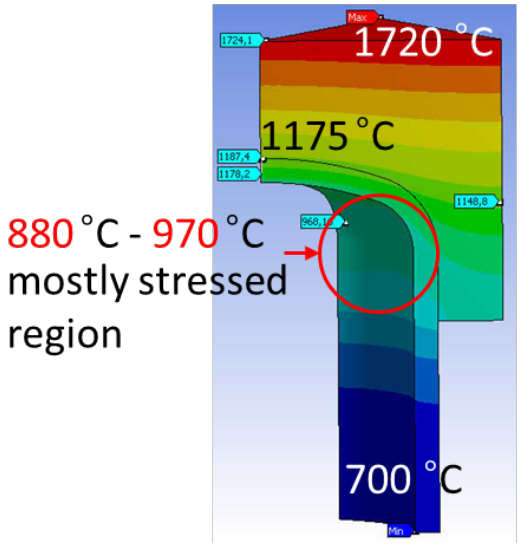

Fig. 17. Temperature field produced in a modular finger target unit (symmetric one sixth part is modelled) computed by a thermo-hydraulic FEA [39].

The temperature field imposes a strong restriction on the operation condition of this target. It is recalled that the structural thimble is subject to two types of temperature limit at the same time to avoid brittleness, that is, DBTT (lower bound: 950 °C) and the recrystallization temperature (upper bound: ca. 1300 °C). This requirement can only be met, if the applied heat flux and the coolant temperature are accurately fixed as defined in Fig. 17. This circumstance means a significant restriction of operational flexibility. Any minor fluctuation in the heat flux load, no matter whether decrease or increase, would lead to a deviation from the prescribed temperature limits.

Another engineering challenge is the requirement to use a reduced activation ODS (oxide dispersion strengthened) steel for the casing and the lead pipe which are joined to the tungsten heat sink. It is noted that the upper service temperature of reduced activation steels (e.g. F82H or Eurofer) is limited to 550 °C due to thermal softening [40]. Obviously, this temperature is by far too low for the lead pipe or casing in the coolant outlet region, thus raising the need of a ODS steel.

It is expected that advanced ODS ferritic Cr steels will be applicable up to 650 °C or possibly even to 700 °C [40]. Yet, the current state-of-the-art is still at a low technological readiness level, particularly, with regard to large-scale metallurgical fabrication and joining [41]. The tight limitation in the upper service temperature of ODS steels (650-700 °C) implies that there

would be actually no design margin to any thermal overshoot due to heat flux fluctuations from the plasma.

6. Conclusions

In this article we overviewed key design requirements and materials issues in view of divertor target development for DEMO reactor. Emphasis was placed on the design considerations to assure the structural reliability under intense neutron irradiation. As reference examples for this review study, two representative target concepts (water- and helium-cooled, respectively) were considered where only the baseline materials are used.

One of the key conclusions of this study is the fact that the structural design requirements and the performance of (irradiated) materials impose mutual impacts on each other. The reason is owing to the constraint that the currently available baseline materials are not able to fulfill the design requirements to a full extent for application to DEMO divertor. This condition demands an iterative, evolutionary and integrated design approach with the option of novel materials. A logical framework of design/material interface needs to be established on the basis of up-to-date metallurgical progress with the support of accumulating materials database and dedicated irradiation campaigns.

In the following some of the technical findings are summarized:

1. Slow transient events with heat flux loads up to 20 MW/m² could be accommodated, when a water-cooled target is employed with a low coolant temperature ($T \leq 150$ °C).
2. At this desired water coolant temperature (150 °C), the maximum allowable stationary heat flux load will be limited to 10 MW/m² or slightly higher at which the structural design rules and the corrosion limit are not violated.
3. There are urgent R&D needs to improve the high-temperature strength and corrosion resistance of water-cooled heat sinks. This is a prerequisite for achieving enhanced HHF capability. Advanced Cu-based composite materials will need to replace CuCrZr alloy.
4. Dedicated structural design criteria for brittle (or embrittled) metals are needed for the target operation at low water-coolant temperature (150 °C) where the irradiated damage of CuCrZr alloy will not be recovered.
5. The design of the helium-cooled modular finger target concept is optimized at the heat flux load of 10 MW/m² with little thermal flexibility and rather optimistic assumptions on materials performance. Any major deviation from the prescribed HHF load, either increase or decrease, would lead to critical deterioration of the structural materials (tungsten, steel).

6. The currently available structural materials (tungsten alloy, Eurofer steel, ODS Eurofer steel) would not allow the application of a helium-cooled divertor target for DEMO, unless the occurrence of any slow transient event can be completely suppressed producing no heat flux overshoots and radiation-resistant tungsten materials have been developed.
7. A helium-cooled divertor target for DEMO might have a chance, only if an innovative design concept with a sufficient operational margin and reliable structural materials with a low DBTT and high toughness are devised.

Acknowledgment

This work has been carried out within the framework of the EUROfusion Consortium and has received funding from the European Union's Horizon 2020 research and innovation programme under grant agreement number 633053. The views and opinions expressed herein do not necessarily reflect those of the European Commission.

References

[1] Romanelli F. et al. 2012 Fusion Electricity-A roadmap to the realization of fusion energy, European Fusion Development Agreement
[2] Stork D. et al. 2014 J. Nucl. Mater. **455** 277-291.
[3] Frosi P. et al. 2014 Draft of load specification for divertor cassette and steel supporting structure for vertical target and dome Report DIV-1.3.2-01 EUROfusion
[4] Gavila P. 2011 Fusion Eng. Des. **86** 1652–1655
[5] Federici G. Private communication
[6] Merola M. et al. 2010 Fusion Eng. Des. **85** 2312–2322
[7] Raffray A.R. et al. 2010 Fusion Eng. Des. **85** 93–108
[8] Mayer M. et al. 2009 Phys. Scr. **T138** 014039
[9] Federici G. et al. 2002 Fusion Eng. Des. 61-62 81-94
[10] Pitts R.A. et al. 2013 J. Nucl. Mater. **438** S48
[11] Igitkhanov Yu. et al. 2013 Design strategy for the PFC in DEMO reactor KIT Scientific Reports 7637 KIT Scientific Publishing
[12] Wenninger R.P. et al. 2014 Nucl. Fusion **54** 114003
[13] Linke J. 2005 Fusion Sci. Tech. **47** 678-685
[14] Li M. et al. 2015 Nucl. Mater. Energy **2** 1-11
[15] Gavila P. et al. 2011 Fusion Eng. Des. **86** 1652-1655
[16] Timmis W. 2013 EFDA Report WP12-MAT02-M03 Copper alloys

[17] Gilbert M.R. et al. 2012 Nucl. Fusion **52** 083019

[18] Benson Ch. et al. 2009 The periodic table of the elements and their chemical properties MindMelder.com

[19] Singh B.N. et al. 2002 J. Nucl. Mater. **307**-**311** 159-170

[20] Edwards D.J. et al. 2005 J. Nucl. Mater. **342** 164-178

[21] Fabritsiev S.A. et al. 1996 J. Nucl. Mater. **233-237** 127-137

[22] Fenici P. et al. 1994 J. Nucl. Mater. **212-215** 399-403

[23] Li M. et al. 2009 J. Nucl. Mater. **393** 36-46

[24] ITER, ITER structural design criteria for in-vessel components (SDC-IC), G 74 MA 8 01-05-28 W0.2 Appendix A Materials design limit data

[25] Wikman S. et al. 2012 EFDA Report Experimental assessment of erosion corrosion parameters of CuCrZr and CuCrZr/316L(N)-IG joints at simulated plasma and nominal operational ITER conditions

[26] Zheng J.H. et al. 2002 Fusion Eng. Des. **61**-**62** 649-657

[27] Belous V. et al. 1998 J. Nucl. Mater. **258**-**263** 351-356

[28] Edwards D.J. et al. 2002 J. Nucl. Mater. **307**-**311** 439-443

[29] Rieth M. Private communication

[30] Rieth M. et al. 2005 J. Nucl. Mater. **342** 20-25

[31] ITER Materials Properties Handbook ITER Document No. S74 RE1 ITER-AM01-2105

[32] Li M. et al. 2015 Fusion Eng. Des. **90** 88-96

[33] Kalinin G.M. et al. 2007 J. Nucl. Mater. **367**-**370** 920-924

[34] You J.H. et al. 2013 J. Nucl. Mater. **438** 1-6

[35] Kimmig S. et al. 2013 J. Nucl. Mater. **440** 272-277

[36] Pintsuk G. et al. 2013 Fusion Eng. Des. **88** 1858-1861

[37] Li M. et al. 2014 Fusion Eng. Des. **89** 2716–2725

[38] Fabritsiev S.A. et al. 1997 Plasma Dev. Operations **5** 133-141

[39] Norajitra P. 2011 Divertor development for a future fusion power plant, Ph.D Thesis, Karlsruher Institut für Technologie, KIT Scientific Publishing

[40] Sandim H.R.Z. et al. 2010 Mater. Sci. Eng. A **527** 3602-3608

[41] Chehtov T. et al. 2007 J. Nucl. Mater. **367**-**370** 1228-1232

Figure captions

Fig. 1. Early version of the CAD model of the DEMO divertor cassette [3].

Fig. 2. Pure materials in solid state which possess thermal conductivity higher than 50 MW/mK. In each box the value of conductivity is given. The grey-shaded boxes indicate the materials that fail to meet at least one or two of the criteria. The 'failed' item of the criteria is indicated on the top of the individual boxes, respectively.

Fig. 3 Uniform elongation data of CuCrZr alloy irradiated to 1-10 dpa plotted as a function temperature. The data were collated from several different test reports published in literature [21-24].

Fig. 4 shows the tensile curves of precipitation-hardened CuCrZr alloy measured before and after irradiation to 10 dpa at 150 °C and 250 °C, respectively (each test temperature is equal to the irradiation temperature) [22].

Fig. 5. Selected stress limits of CuCrZr alloy from the SDC-IC code plotted as a function of temperature. The subscript 'irr' and 'unirr' stands for the data of an irradiated and pristine specimen, respectively [24].

Fig. 6. Fracture energy of cold-irradiated (80 °C) CuCrZr alloy with two different kinds of heat treatment as a function of irradiation dose (SAA: solution-annealed & prime aged, SCA: slow-cooled & aged) [22].

Fig. 7. Data of Charpy impact tests conducted for pure W, La oxide-doped tungsten (WL10), a reduced-activation steel (9Cr-1WVTa) and a Mo alloy (TZM) [30].

Fig. 8. Mock-up of an ITER divertor target element consisting of tungsten monoblocks joined with a CuCrZr cooling tube via a Cu interlayer [13].

Fig. 9. Schematic of the FEA model (symmetric half) considered for FEA. W armor block: 23 mm×22 mm×4 mm, cooling tube thickness: 1 mm, inner diameter: 12 mm, Cu interlayer thickness: 0.5 mm.

Fig. 10. Temperature field in the cooling tube (left half part) predicted for the heat flux load of 15 MW/m² and coolant temperature of 200 °C. The two locations are indicated for which the temperature values are presented [32].

Fig. 11. Circumferential component of the thermal stress field produced in the cooling tube after 10 load cycles (heat flux load: 15 MW/m², coolant temperature of 200 °C).

Fig. 12. Circumferential (left) and axial (right) component of the plastic strain in the cooling tube after 10 load cycles (heat flux load: 15 MW/m², coolant temperature of 200 °C) [32].

Fig. 13. History of the principal plastic strain components in the cooling tube bulk during the HHF load cycles (cylindrical coordinate system). The fabrication process and pre-heating to standby state are also considered [32].

Fig. 14. History of the principal plastic strain components in the copper interlayer during the HHF load cycles. The fabrication process and pre-heating to standby state are also considered [32].

Fig. 15. Longitudinal section view of a multi-jet modular finger target unit with a schematic illustration (left) and photograph (right) [39].

Fig. 16. Heat sink (thimble) of the modular finger target made of tungsten alloy (WL10) which is subjected to pressurized hot helium gas (600 - 700 °C, 100 bar) [39].

Fig. 17. Temperature field produced in a modular finger target unit (symmetric one sixth part is modelled) computed by a thermo-hydraulic FEA [39].

Table 1. Temperatures (°C) at two selected locations of the cooling tube computed by FEA.

Heat flux load	10 MW/m²		15 MW/m²		18 MW/m²	
Coolant water	150	200	150	200	150	200
Tube top bond interface	263	308	316	351	348	378
Tube top inner wall	229	274	266	300	288	317
Tube side bond interface	172	220	181	228	187	233
Tube side inner wall	169	217	177	225	182	229